Plasma Sources Sci. Technol. **17** (2008) 024016 (10pp) doi:10.1088/0963-0252/17/2/024016

Energizing and depletion of neutrals by a collisional plasma

A Fruchtman

H.I.T.—Holon Institute of Technology, 52 Golomb Street, Holon 58102, Israel

Received 30 October 2007, in final form 10 March 2008
Published 1 May 2008
Online at stacks.iop.org/PSST/17/024016

Abstract
Neutral depletion can significantly affect the steady state of low temperature plasmas. Recent theoretical analyses predicted previously unexpected effects of neutral depletion in both collisional and collisionless regimes. In this paper we address the effect of the energy deposited in the neutral gas by a collisional plasma. The fraction of power deposited in the neutrals is shown to be independent of the amount of power. The first case we address is of a thermalized neutral gas. It is shown that a low heat conductivity of the neutral gas is followed by a high neutral temperature that results in a high neutral depletion even if the plasma pressure is small. In the second case neutrals are accelerated through charge exchange with ions leading to what we call neutral pumping, which is equivalent to ion pumping in a collisionless plasma. Neutral depletion is found in the second case for both a closed system (no net mass flow) and an open system (a finite mass flow). A thruster that employs a collisional plasma and pumped neutrals is compared with the thruster analyzed before that employs collisionless plasma.

1. Introduction

Space and laboratory plasmas can be significantly affected by neutral depletion. In weakly ionized laboratory plasmas, in which the neutral density and temperature are uniform, particle balance is decoupled from power balance and the electron temperature is found to be related to a single similarity variable, the product of the neutral gas pressure and the plasma spatial extent (the Paschen parameter) [1–6]. The plasma density is determined by power balance and increases monotonically with deposited energy, as does the plasma flux. When ionization is intense and neutral depletion is significant, so that neutral pressure is not uniform, the above-mentioned similarity variable is no longer well defined. Moreover, particle balance and power balance become coupled and so do ionization and transport.

The effect of neutral depletion in gas discharges has already been addressed in early studies [7–10]. However, only in recent years, with the growing use of lower pressure and higher power radio-frequency discharges, has the importance of neutral depletion become fully recognized [11–30]. Decrease in the neutral density [11–13, 15, 19–21, 23], relaxation oscillations [14] and neutral-gas heating [16–20, 22, 23] have been measured. Several recent theoretical studies focused on the effect of neutral depletion on the steady state of low temperature plasmas [24–30]. In these studies the total number of neutrals has been found to replace the Paschen parameter as the similarity variable that determines the electron temperature. For collisional plasma that is in pressure balance with the neutral gas it has been shown that because of the inherent coupling of ionization and transport, an increase in the energy invested in ionization can nonlinearly enhance the transport process. Such an enhancement of the plasma transport due to neutral depletion was shown to result in an unexpected decrease in the plasma density when power is increased despite the increase in the flux of generated plasma [24]. An unexpected feature of the steady state has also been found for collisionless plasma interacting through ionization only with thermalized neutral gas. Strong ionization was found to result in a maximum of the neutral-gas density surprisingly located at the center of the chamber [27]. For collisionless neutral gas, however, the strong ionization resulted in the expected neutral-gas minimum at the center of the chamber [25, 26]. We have recently studied in detail this case of collisionless neutral-gas interacting with a collisionless plasma [30]. We analyzed the steady state of such plasma and neutral gas in both zero and finite mass flow configurations. The configuration with a net mass flow was considered for a thruster. The energy cost for ionization and the backwall energy losses were shown to significantly reduce the efficiency of such a thruster.

In this paper we address the effect of the energy deposited in the neutral gas by a collisional plasma. In section 2 we derive relations between the plasma flow, density and velocity that are independent of deposited power and the neutral density profile. Moreover, in section 3 we show that the fraction of power deposited in the neutrals is also independent of the amount of deposited power and of the neutral density profile, and is determined by the atomic cross sections and by the electron temperature only.

The first case we address is of a thermalized neutral gas in which the neutral-gas pressure is expressed as the product of the density and temperature. This case is analyzed in sections 4 and 5. In section 4 we write the heat equation that governs the evolution of the neutral-gas temperature. Neutral heating is balanced by heat conduction to the boundaries. This case was recently analyzed [29] where the source of gas heating was assumed to be collisions with plasma electrons. We allow both work done by the plasma flow and heat produced by collisions with electrons to contribute to the increase in electron temperature. In section 5 we examine in detail the role of neutral heat conductivity. In the numerical examples we retain only heating due to collisions with electrons, as was done in [29]. For a small coefficient of neutral heat conductivity we derive asymptotic relations. We show that a low heat conductivity of the neutral gas is followed by a high neutral temperature that results in a high neutral depletion even if the plasma pressure is small.

In the second case, described in sections 6–8, neutrals (that move ballistically as in our recent paper [30]) are accelerated through charge-exchange collisions with fast ions, leading to what we call neutral pumping. This neutral pumping is equivalent to ion pumping in collisionless plasmas that results from intense ionization [12–14]. The fast neutrals generated in the charge-exchange collisions are assumed to leave the system quickly, and, because of their short residence time, they are assumed not to be ionized. This simplified formalism for neutral depletion due to neutral pumping is presented in section 6. A closed system in which neutral pumping is dominant is analyzed in section 7. An open system with a net mass flow is analyzed in section 8. This analysis has relevance to plasma sources that are considered for use as thrusters [31–40]. A thruster that employs a collisional plasma and pumped neutrals could be advantageous relative to a similar thruster that employs collisionless plasma [30]. The analysis here is too simplified for making the needed comparison. We nevertheless discuss such a collisional thruster in section 8.

2. Collisional plasma

In this section we derive for a collisional plasma relations between the flow, velocity and density that are independent of the neutral density profile. We assume a one-dimensional unmagnetized plasma. The momentum equations for the electrons and ions are

$$\frac{\mathrm{d}\,(nT)}{\mathrm{d}z} = -neE - m_\mathrm{e}\beta_\mathrm{e}Nnv, \qquad \frac{\mathrm{d}\left(mnv^2\right)}{\mathrm{d}z} = neE - m\beta_\mathrm{i}Nnv. \tag{1}$$

Here n is the density of the quasi-neutral plasma, T is the (assumed constant) electron temperature, e the elementary charge, E the intensity of the ambipolar electric field, m and m_e the ion and electron masses, v the velocity of the plasma flow and N the density of the neutrals. Also, β_e and β_i are the rate coefficients of electron and ion collisions with neutrals.

Adding the two momentum equations we obtain the standard collisional plasma momentum equation:

$$\frac{\mathrm{d}\left(mnv^2+nT\right)}{\mathrm{d}z} = -m\beta_\mathrm{c}Nnv, \qquad \beta_\mathrm{c} \equiv \beta_\mathrm{i} + \beta_\mathrm{e1}, \qquad \beta_\mathrm{e1} \equiv \beta_\mathrm{e}\frac{m_\mathrm{e}}{m}. \tag{2}$$

The continuity equation is

$$\frac{\mathrm{d}\Gamma}{\mathrm{d}z} = \beta Nn, \qquad \Gamma \equiv nv, \tag{3}$$

in which $\beta = \beta(T)$ is the ionization rate coefficient and Γ is the plasma particle flux density. Combining the two equations we obtain the relation

$$\frac{\mathrm{d}\left(mnv^2+nT\right)}{\mathrm{d}\Gamma} = -\frac{m\beta_\mathrm{c}}{\beta}v. \tag{4}$$

This equation can be written in the form

$$\frac{\mathrm{d}\ln\Gamma}{\mathrm{d}M^2} = \frac{(1-M^2)}{2M^2[1+M^2(1+\beta_\mathrm{c}/\beta)]}, \tag{5}$$

in which

$$M \equiv \frac{v}{c} \tag{6}$$

is the Mach number and $c \equiv (T/m)^{1/2}$ is the ion acoustic velocity. Equation (5) shows that the flux does not grow with the velocity beyond $M = 1$. We assume that the Mach number is unity at the plasma boundary. The equation is integrated and the plasma flux and density are expressed as

$$\Gamma = ncM, \qquad n = \frac{n_0}{[1+M^2(1+\beta_\mathrm{c}/\beta)]^{\frac{1}{2}(1+\frac{1}{1+\beta_\mathrm{c}/\beta})}}. \tag{7}$$

Here n_0 is the maximal plasma density (where the plasma flow velocity is zero). The maximal plasma flux and the minimal plasma density, both at the plasma boundary, are

$$\Gamma_\mathrm{max} = n_\mathrm{min}c, \qquad n_\mathrm{min} = \frac{n_0}{(2+\beta_\mathrm{c}/\beta)^{\frac{1}{2}(1+\frac{1}{1+\beta_\mathrm{c}/\beta})}}. \tag{8}$$

The effect of neutral depletion on the collisionless case, in which

$$\beta_\mathrm{c} = 0 \Longrightarrow n = \frac{n_0}{(1+M^2)}, \qquad \Gamma_\mathrm{max} = \frac{n_0 c}{2}, \qquad n_\mathrm{min} = \frac{n_0}{2}, \tag{9}$$

has been analyzed in [30]. We are interested here in the collisional case, in which

$$\beta_\mathrm{c} \gg \beta. \tag{10}$$

For each ionization event there are several collisions in which neutrals acquire momentum. In that case we approximate

$$\beta_c \gg \beta \Longrightarrow n = \frac{n_0}{[1+M^2(\beta_c/\beta)]^{\frac{1}{2}}},$$
$$\Gamma = \frac{n_0 c M}{[1+M^2(\beta_c/\beta)]^{\frac{1}{2}}}. \tag{11}$$

We will use equations (11) in this paper with the normalized plasma flux Γ_n and density n_n satisfying the following relations:

$$\Gamma_n^2 = 1 - n_n^2, \qquad \Gamma_n \equiv \frac{\Gamma}{\Gamma_a}, \qquad n_n \equiv \frac{n}{n_0}, \tag{12}$$

where

$$\Gamma_a \equiv n_0 c \left(\frac{\beta}{\beta_c}\right)^{1/2}. \tag{13}$$

Relations (11) and (12) can be obtained by neglecting the ion inertia in the ion momentum equation from the outset. Although the plasma velocity increases monotonically with the plasma flux once the ion inertia has been neglected, the simplified collisional model is valid only for Mach numbers up to $M = 1$, where

$$n = n_{\min} \cong n_0 \left(\frac{\beta}{\beta_c}\right)^{1/2}, \quad \Gamma = \Gamma_{\max} \cong \Gamma_a \left(1 - \frac{\beta}{2\beta_c}\right). \tag{14}$$

It is necessary to retain the small term $\beta/(2\beta_c)$ in the expression for $\Gamma_{\max}$ for the calculation of the neutral-gas heating, as described in the following section. The simple relation between the plasma flux density and the plasma density (equations (12)) is used here for deriving from the continuity equation an expression for N_T , the total number of neutrals (per unit area) between the location of the peak of plasma density (at $z = 0$) and the plasma boundary (located at $z = a$):

$$N_T = \int_0^a N\,\mathrm{d}z = \frac{c}{(\beta\beta_c)^{1/2}} \int_0^{1-\beta/(2\beta_c)} \frac{\mathrm{d}\Gamma_n}{(1-\Gamma_n^2)^{1/2}}$$
$$\cong \frac{\pi}{2}\frac{c}{(\beta\beta_c)^{1/2}}. \tag{15}$$

This last relation exhibits what has been pointed out recently [24, 27, 30]: N_T, the total number of neutrals, determines the electron temperature. The total number of neutrals is the same in the two regions between the plasma maximal density and the two opposing boundaries, even if the peak plasma density is not at the middle plane between those two boundaries.

In the following section we will calculate the potential drop across the plasma and the power deposited in the neutrals by the plasma.

3. Plasma potential and power deposited in the neutrals

The potential difference across the plasma (the potential at $\Gamma = 0$ taken as zero) is

$$\varphi(z) = -\int_0^z E\,\mathrm{d}z' = -\int_0^z \frac{m}{e}\frac{\beta_i}{\beta}\frac{\mathrm{d}\Gamma}{\mathrm{d}z'}\frac{v}{n}\mathrm{d}z' = \frac{T}{e}\frac{\beta_i}{\beta_c}\ln n_n(z). \tag{16}$$

Note that this result is independent of the neutral density. This is a Boltzmann relation modified by collisions. If the electrons are collisionless, $\beta_i = \beta_c$, the usual Boltzmann relation is recovered. Using equation (14) for the plasma density at the boundary, we find that the potential difference across the quasi-neutral plasma is

$$\Delta\varphi = \frac{T}{e}\frac{\beta_i}{\beta_c}\ln n_{n,\min} \cong -\frac{T}{e}\frac{\beta_i}{\beta_c}\ln\frac{\beta_c}{\beta}. \tag{17}$$

Let us discuss now the energy deposited in the neutrals due to their interaction with plasma particles. The power per unit volume $p_N(z)$ is composed of several sources, as described in [29], based on [4, 41]:

$$p_N(z) = p_{NQe}(z) + p_{NQi}(z) + p_{Nwe}(z) + p_{Nwi}(z), \tag{18}$$

where

$$p_{NQe} = 3nN\beta_{e1}(T - T_g), \qquad p_{NQi} = \tfrac{3}{4}nN\beta_i(T_i - T_g),$$
$$p_{Nwe} = Nnm_e\beta_e v^2, \qquad p_{Nwi} = Nnm\beta_i v^2. \tag{19}$$

The first two terms express neutral heating due to collisions with electrons and ions and the last two terms the work done on the neutrals by the electron and the ion flows. Here T_g is the neutral-gas temperature. We assume that the neutral and ion temperatures are much smaller than the electron temperature

$$T_g, T_i \ll T. \tag{20}$$

We therefore neglect p_{NQi} and approximate $p_{NQe} = 3nN\beta_{e1}T$. The various sources of neutral heating are therefore approximated as

$$p_{NQe} = 3nN\beta_{e1}T, \qquad p_{NQi} = 0,$$
$$p_{Nwe} = Nnm_e\beta_e v^2, \qquad p_{Nwi} = Nnm\beta_i v^2. \tag{21}$$

The power per unit volume can be integrated along the flow. The power deposited in the neutrals due to the work done by the ions, P_{Nwi}, and by the electrons, P_{Nwe}, is

$$P_{Nwi,e}(z) = \int_0^z p_{Nwi,e}(z')\,\mathrm{d}z' = \int_0^z m\frac{\beta_{i,e1}}{\beta}\frac{\mathrm{d}\Gamma}{\mathrm{d}z'}v^2\,\mathrm{d}z'$$
$$= \Gamma_a T\frac{\beta_{i,e1}}{\beta_c}\left[\ln\sqrt{\frac{1+\Gamma_n(z)}{1-\Gamma_n(z)}} - \Gamma_n(z)\right]. \tag{22}$$

In order to calculate the power $P_{Nwi,e}(a)$ we use the value of the normalized plasma flux at the plasma edge (14), $\Gamma_n(a) = 1 - \beta/(2\beta_c)$, in which we must retain the small term $\beta/(2\beta_c)$; otherwise the power is infinite. The total power deposited in the neutrals due to the work by both ions and electrons turns out to be

$$P_{Nw}(a) = P_{Nwi}(a) + P_{Nwe}(a) \cong \Gamma_a\frac{T}{2}\ln\frac{\beta_c}{\beta}. \tag{23}$$

This power is independent of the neutral density. The power per plasma particle is determined by the atomic cross sections (β_c/β) and by the electron temperature only. We note that

$$P_{Nw}(a) \cong -\frac{1}{2}\frac{\beta_c}{\beta_i}\Gamma_a e\Delta\varphi. \tag{24}$$

The distribution of ionization is such that on average an ion gains (and delivers to the neutrals) **half** of the electric energy available due to the voltage drop across the plasma.

The power deposited in the neutrals due to their collisions with electrons is

$$P_{NQe}(z) = \int_0^z p_{NQe}(z')\,dz' = 3\beta_{e1}T\int_0^z Nn\,dz' = 3\frac{\beta_{e1}}{\beta}T\int_0^\Gamma d\Gamma'. \quad (25)$$

The total heating is obtained, for $\Gamma(a) \cong \Gamma_a$, as

$$P_{NQe}(a) = 3\frac{\beta_{e1}}{\beta}\Gamma_a T. \quad (26)$$

The total power deposited in the neutrals is therefore

$$P_N(a) = P_{Nw}(a) + P_{NQe}(a) \cong \Gamma_a T\left(\frac{1}{2}\ln\frac{\beta_c}{\beta} + 3\frac{\beta_{e1}}{\beta}\right), \quad (27)$$

where $P_N(z) \equiv P_{Nw}(z) + P_{NQe}(z)$. Our previous observation is true also for the total power deposited in the neutrals: the rate of neutral heating by one particle of plasma depends only on the electron temperature and on the atomic rate coefficients. It is independent of the neutral density. In the collisional regime, $\beta_c \gg \beta$, the rate of heating due to collisions with ions depends only logarithmically on the large ratio of the collision to ionization frequencies. If β_c and β_{e1} are comparable, the heating by the electrons is dominant, as is indeed assumed in [29]. The neutral heating by the work done by the ions is expected to be larger when their collisions are described by Godyak's model [3]. This case will be addressed in a future study.

In the following section we examine the evolution of the neutral temperature in a thermalized neutral gas.

4. Thermalized neutral gas

In this section we assume that the neutral-gas pressure is a scalar $N(z)T_g(z)$, where $T_g(z)$ is the neutral-gas temperature. The evolution of the neutral-gas temperature is governed by the following energy equation:

$$\frac{d}{dz}\left[K(T_g)\frac{dT_g}{dz}\right] = -p_N(z) = -nN(3\beta_{e1}T + m\beta_c v^2), \quad (28)$$

as was described in [29] based on [4, 41]. Here $K(T_g)$ is the coefficient of heat conductivity. In the equation we used the approximations for $p_N(z)$ from the previous section. Since ion inertia has been neglected pressure balance between ions and neutral gas holds:

$$P_r = NT_g + nT, \quad (29)$$

where P_r is the uniform total pressure. Power balance is written as

$$P = \varepsilon_T(T)\Gamma(z=a) - K(T_g)\frac{dT_g}{dz}(z=a), \quad (30)$$

where P is the power deposited per unit area in both plasma and neutrals. Power balance includes the energy deposited in the plasma $\varepsilon_T(T_e)$, which is the energy cost for an ion–electron pair production excluding neutral-gas heating [4], and in the neutral gas. Walls are symmetrically located at $z = \pm a$. The specified P_r, P, a, cross sections $\beta_i(T)$, $\beta_e(T)$ and β_c, and boundary conditions $T_g(z=\pm a) = T_{gW}$ and $n(z=\pm a) \cong 0$, could determine the profiles in z of n, Γ, N, and T_g and the uniform value of T.

Using the expressions in the previous section we write

$$K(T_g)\frac{dT_g}{dz} = -P_N(z) = -\Gamma_a T\left[\ln\sqrt{\frac{1+\Gamma_n(z)}{1-\Gamma_n(z)}} - \Gamma_n(z) + 3\frac{\beta_{e1}}{\beta}\Gamma_n(z)\right]. \quad (31)$$

With the continuity equation we express the equation as

$$\frac{K}{T_g}\frac{dT_g}{d\Gamma_n} = -\frac{c^2}{\beta_c(P_r/n_0T - n_n)n_n} \times\left[\ln\sqrt{\frac{1+\Gamma_n(z)}{1-\Gamma_n(z)}} + \left(3\frac{\beta_{e1}}{\beta} - 1\right)\Gamma_n(z)\right]. \quad (32)$$

We assume for simplicity that

$$K(T_g) = K = \text{const} \quad (33)$$

and derive the following expression for the neutral-gas temperature:

$$T_g = \frac{T_{gw}}{(1-\sin\theta_0\cos\theta)^{1/K_e}} \times\exp\left[\frac{\sin\theta_0}{K_i}\int_\theta^{\theta_{max}}\frac{d\theta'}{(1-\sin\theta_0\cos\theta')}\ln\sqrt{\frac{1+\sin\theta'}{1-\sin\theta'}}\right], \quad (34)$$

where T_{gw} is the neutral-gas temperature at the wall, and

$$\theta \equiv \arcsin\Gamma_n, \qquad \theta_{max} = \frac{\pi}{2} - \sqrt{\frac{\beta}{\beta_c}}, \qquad \sin\theta_0 \equiv \frac{n_0T}{P_r},$$
$$K_i \equiv \frac{K\beta_c}{c^2}, \qquad K_e \equiv \frac{K_i}{3\beta_{e1}/\beta - 1}. \quad (35)$$

The maximal neutral-gas temperature (at the plasma center) is found to be

$$T_{g0} = T_g(\theta=0) = \frac{T_{gw}}{(1-\sin\theta_0)^{1/K_e}} \times\exp\left[\frac{\sin\theta_0}{K_i}\int_0^{\theta_{max}}\frac{d\theta'}{(1-\sin\theta_0\cos\theta')}\ln\sqrt{\frac{1+\sin\theta'}{1-\sin\theta'}}\right]. \quad (36)$$

We now express the neutral density as

$$N = \frac{P_r}{T_g}(1-\sin\theta_0\cos\theta). \quad (37)$$

The continuity equation becomes

$$\frac{d\theta}{d\xi} = \alpha_L^{1/2}(1-\sin\theta_0\cos\theta)^{1+1/K_e} \times\exp\left[\frac{\sin\theta_0}{K_i}\int_\theta^{\theta_{max}}\frac{d\theta'}{(1-\sin\theta_0\cos\theta')}\ln\sqrt{\frac{1+\sin\theta'}{1-\sin\theta'}}\right], \quad (38)$$

where

$$\alpha_L^{1/2} \equiv \frac{(\beta\beta_c)^{1/2} N_w a}{c}, \qquad \xi \equiv \frac{z}{a} \qquad N_w \equiv \frac{P_r}{T_{gw}}. \tag{39}$$

Equation (38) is reduced to the equation used in [24] once the conductivity is infinite ($K_i, K_e \longrightarrow \infty$). Integrating equation (38) we obtain

$$\alpha_L^{1/2}\xi = \int_0^{\theta} \frac{d\theta'}{(1-\sin\theta_0\cos\theta')^{1+1/K_e}} \times \exp\left[-\frac{\sin\theta_0}{K_i}\int_{\theta'}^{\theta_{max}} \frac{d\theta''}{(1-\sin\theta_0\cos\theta'')} \ln\sqrt{\frac{1+\sin\theta''}{1-\sin\theta''}}\right]. \tag{40}$$

Integrating equation (40) until the wall we obtain the following relation:

$$\alpha_L^{1/2} = \int_0^{\theta_{max}} \frac{d\theta}{(1-\sin\theta_0\cos\theta)^{1+1/K_e}} \times \exp\left[-\frac{\sin\theta_0}{K_i}\int_{\theta}^{\theta_{max}} \frac{d\theta'}{(1-\sin\theta_0\cos\theta')} \ln\sqrt{\frac{1+\sin\theta'}{1-\sin\theta'}}\right], \tag{41}$$

which should be added to the previous relation (30). In the case of a small plasma pressure, $\sin\theta_0 \ll 1$, the last equation is reduced to Schottky's case: $\alpha_L^{1/2} \cong \pi/2$ [1].

Once these equations are solved we can calculate the neutral depletion as defined in [30]:

$$D \equiv \frac{N(a)-N(0)}{N(0)}. \tag{42}$$

In our case the neutral depletion turns out to be

$$D = \frac{1}{(1-\sin\theta_0)^{1+1/K_e}} \times \exp\left[\frac{\sin\theta_0}{K_i}\int_0^{\theta_{max}} \frac{d\theta}{(1-\sin\theta_0\cos\theta)} \ln\sqrt{\frac{1+\sin\theta}{1-\sin\theta}}\right] - 1. \tag{43}$$

In the following section we examine how the magnitude of the heat conductivity affects the plasma and the neutral steady state.

5. The effect of heat conductivity

Following the discussion at the end of section 3, and as was done in [29], we examine the case that the electron heating is dominant. Equations (40) and (41) are reduced to

$$\alpha_L^{1/2}\xi = \int_0^{\theta} \frac{d\theta'}{(1-\sin\theta_0\cos\theta')^{1+1/K_e}}, \tag{44}$$

and to

$$\alpha_L^{1/2} = \int_0^{\pi/2} \frac{d\theta}{(1-\sin\theta_0\cos\theta)^{1+1/K_e}}. \tag{45}$$

Here θ_{max} is approximated as $\pi/2$. Cases with finite values of K_e were presented in [29]. We present analytical results for $K_e = \infty$, as in [24] and in [27], and also for $K_e = 1$ and $K_e \ll 1$.

In the case that $K_e = \infty$ equations (44) and (45) are integrated, as in [24], to

$$\frac{\cos\theta - \sin\theta_0}{\sin\theta\cos\theta_0} = \cot[(\alpha_L^{1/2}\cos\theta_0)\xi], \tag{46}$$

and to

$$\alpha_L^{1/2}\cos\theta_0 = \frac{\pi}{2} + \theta_0. \tag{47}$$

This last equation is in the form of Kepler's equation.

The special case $K_e = 1$ can also be integrated as follows:

$$\alpha_L^{1/2}\xi = \int_0^{\theta} \frac{d\theta'}{(1-\sin\theta_0\cos\theta')^2} = \frac{1}{\cos^3\theta_0} \times \left\{2\arctan\left[\frac{(1+\sin\theta_0)\tan(\theta/2)}{\cos\theta_0}\right] + \frac{\sin\theta_0\cos\theta_0\sin\theta}{1-\sin\theta_0\cos\theta}\right\}. \tag{48}$$

Using equation (45) for $K_e = 1$ in its form in equation (48) we obtain the relation

$$\alpha_L^{1/2}\cos^3\theta_0 = \frac{\pi}{2} + \theta_0 + \sin\theta_0\cos\theta_0. \tag{49}$$

Let us discuss the evaluation of integral (45) for the case of a low heat conductivity, $K_e \ll 1$. We write the integral as

$$\alpha_L^{1/2} = \int_0^{\pi/2} d\theta' \exp\left[\frac{h(\theta')}{\varepsilon}\right], \tag{50}$$

where

$$\frac{1}{\varepsilon} \equiv 1 + \frac{1}{K_e}, \qquad h(\theta) \equiv -\ln(1-\sin\theta_0\cos\theta). \tag{51}$$

Since $h(\theta)$ is a decreasing function in the interval $[0, \pi/2]$ we can employ Laplace's method [42] for a small ε to obtain the asymptotic form of the integral. The derivative $h'(0)$ is zero and the integral becomes

$$\alpha_L^{1/2} = \left[-\frac{\pi\varepsilon}{2h''(0)}\right]^{1/2} \exp\left[\frac{h(0)}{\varepsilon}\right]. \tag{52}$$

Thus, integral (45) at the asymptotic limit $\varepsilon \cong K_e \ll 1$ turns out to be

$$\alpha_L^{1/2} = \left(\frac{\pi K_e}{2\sin\theta_0}\right)^{1/2} \frac{1}{(1-\sin\theta_0)^{1/2+1/K_e}}. \tag{53}$$

Equations (47), (49) and (53) are approximated forms of the eigenvalue equation (45) and relate $\alpha_L^{1/2}$ and θ_0 for different values of K_e.

As numerical examples we present different cases in which the total number of neutrals in the system, the deposited power and the wall temperature T_{gw} are specified and constant. Since the total number of neutrals is fixed the electron temperature T is also fixed, as shown in section 2 (see equation (15)). The total power is fixed and therefore the maximal plasma density n_0 is also fixed, according to equaion (30). For different values of the coefficient of the neutral-gas heat conductivity K_e the profile of the neutral-gas temperature $T_g(z)$ and the total pressure P_r are different. If, for the same number of neutrals and the same amount of deposited power, K_e is smaller,

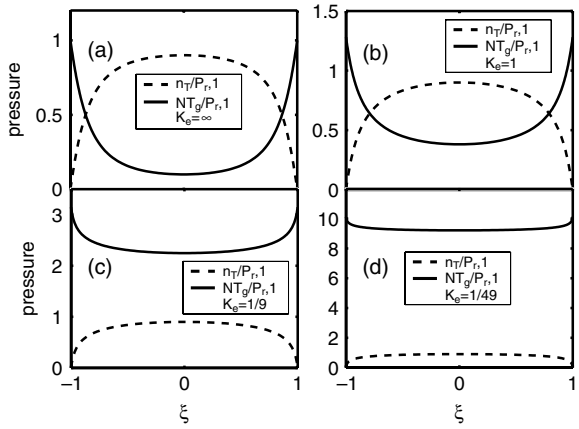

Figure 1. Normalized plasma and neutral pressures for four different coefficients of heat conductivity, K_e. The resulting normalized total pressure $\overline{P_{r,T}}$ is (*a*) $\overline{P_{r,T}} = 1$, (*b*) $\overline{P_{r,T}} = 1.281$, (*c*) $\overline{P_{r,T}} = 3.147$ and (*d*) $\overline{P_{r,T}} = 10.112$.

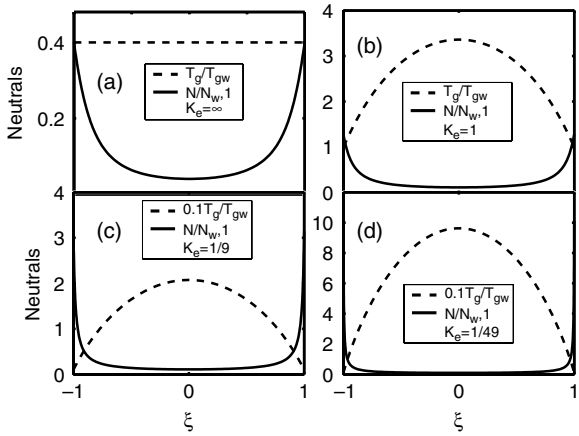

Figure 2. Normalized neutral-gas density and temperature for four different coefficients of heat conductivity, K_e, as in figure 1. The resulting maximal normalized neutral density $\overline{N}(\xi = \pm 1)$ equals the normalized total pressure mentioned in the text. The maximal normalized neutral temperature $T_g(\xi = 0)/T_{gw}$ and the neutral depletion D are (*a*) $T_g(\xi = 0)/T_{gw} = 1$, $D = 9$, (*b*) $T_g(\xi = 0)/T_{gw} = 3.3613$, $D = 10.3$, (*c*) $T_g(\xi = 0)/T_{gw} = 20.73$, $D = 28$ and (*d*) $T_g(\xi = 0)/T_{gw} = 96.29$, $D = 104.7$. Note that in (*c*) and (*d*) $0.1T_g/T_{gw}$ is presented.

$\sin\theta_0$ should be smaller and $\alpha_L^{1/2}$ should be larger, both by the same numerical factor, corresponding to a larger total pressure P_r (see the definitions in equations (35) and (39)). We analyze four cases where $K_e = K_{e,j}$, $\sin\theta_0 = \sin\theta_{0,j}$, $\alpha_L^{1/2} = (\alpha_L^{1/2})_j$ and $P_r = P_{r,j}$ for $j = 1, 2, 3, 4$. We choose for the first case the values

$$K_e = K_{e,1} = \infty \ (\varepsilon = 1) \qquad \sin\theta_0 = \sin\theta_{0,1} = 0.9. \tag{54}$$

Once the values of $K_{e,1}$ and of $\sin\theta_{0,1}$ have been specified, the value of $(\alpha_L^{1/2})_1$ is determined through the integral in equation (45) and is found to be $\alpha_L^{1/2} = (\alpha_L^{1/2})_1 = 6.1726$. The three additional values of K_e are chosen to be $K_{e,2} = 1$ ($\varepsilon = 0.5$), $K_{e,3} = 1/9$ ($\varepsilon = 0.1$), and $K_{e,4} = 1/49$ ($\varepsilon = 0.02$). For each value of K_e we numerically find $\sin\theta_{0,j}$ and $(\alpha_L^{1/2})_j$ that both satisfy equation (45) and the relation

$$\frac{\sin\theta_{0,j}}{\sin\theta_{0,1}} = \frac{(\alpha_L^{1/2})_1}{(\alpha_L^{1/2})_j}. \tag{55}$$

As explained above, this means that, as a result of the different value of K_e, the total pressure is different, satisfying

$$\frac{P_{r,1}}{P_{r,j}} = \frac{\sin\theta_{0,j}}{\sin\theta_{0,1}} = \frac{(\alpha_L^{1/2})_1}{(\alpha_L^{1/2})_j}. \tag{56}$$

For each case the normalized plasma pressure $\overline{P_{rp}} \equiv nT/P_{r,1} = \cos\theta\sin\theta_{0,1}$, normalized neutral-gas temperature $\overline{T_g} \equiv T_g/T_{gw} = (1 - \sin\theta_0\cos\theta)^{-1/K_e}$, normalized neutral-gas density $\overline{N} \equiv NT_{gw}/P_{r,1} = N/N_1(\xi = \pm 1) = (P_{r,j}/P_{r,1})(1-\sin\theta_{0,j}\cos\theta)^{1+1/K_e}$ and normalized neutral-gas pressure $\overline{P_{r,N}} \equiv NT_g/P_{r,1}$ are calculated. The neutral density is normalized to $N_1(\xi \pm 1)$, the neutral density at the wall in the first case, while both plasma and neutral-gas pressures are normalized to the total pressure in the first case. Figure 1 shows the normalized plasma and neutral-gas pressures for the four cases. Figure 2 shows the normalized neutral-gas temperature and density for the four cases. Note that for cases 3 and 4 the temperature divided by 10 is presented. It is seen in the figures that a lower K_e results in a higher T_g, a higher neutral depletion D and a higher total pressure P_r. Even though the plasma pressure becomes *smaller* relative to the total pressure, the larger neutral heating results in a *larger* neutral depletion. The relative plasma pressure is $\sin\theta_{0,1} = 0.9$, $\sin\theta_{0,2} = 0.7025$, $\sin\theta_{0,3} = 0.286$ and $\sin\theta_{0,4} = 0.089$, while the corresponding normalized total pressure $\overline{P_{r,T}} = \overline{P_{rp}} + \overline{P_{r,N}} = \overline{N}(\xi = \pm 1)$ is 1, 1.281, 3.147 and 10.112. The neutral depletion D increases correspondingly and takes the values 9, 10.3, 28 and 104.7. The maximal normalized neutral density $\overline{N}(\xi = \pm 1)$ equals the normalized total pressure, as indicated above.

In this section we have analyzed how the heat conductivity affects the neutral-gas temperature, the neutral depletion and the plasma steady state. In the following section we assume that the neutral gas is mostly affected by charge-exchange collisions.

6. Neutral pumping

We assume that the neutrals move ballistically either to the right (positive z) with a flow of flux density $\Gamma_1(z)$ and density $N_1(z)$ or to the left with a flow of flux density $\Gamma_2(z)$ and density $N_2(z)$. For simplicity, they are all assumed to have a velocity of the same magnitude $v_a = \Gamma_1(z)/N_1(z) = \Gamma_2(z)/N_2(z)$. Part of the neutrals are accelerated through charge-exchange collisions with fast ions. This fast component of the neutral flow is of a flux density $\Gamma_3(z)$ and density $N_3(z)$ and is in the direction of the plasma flow. We call the process of depleting of neutrals through their collisions with ions neutral pumping. Particle conservation is expressed as

$$\Gamma + \Gamma_1 - \Gamma_2 + \Gamma_3 = \Gamma_m, \tag{57}$$

where Γ_m is the total particles flux density and

$$N = N_1 + N_2 + N_3. \tag{58}$$

The continuity equations for the various species are

$$\frac{\mathrm{d}\Gamma}{\mathrm{d}z} = \beta(N_1 + N_2 + N_3)n, \qquad \frac{\mathrm{d}\Gamma_1}{\mathrm{d}z} = -\beta N_1 n - \beta_c N_1 n,$$
$$\frac{\mathrm{d}\Gamma_2}{\mathrm{d}z} = \beta N_2 n + \beta_c N_2 n, \tag{59}$$

and

$$\frac{\mathrm{d}\Gamma_3}{\mathrm{d}z} = \beta_c(N_1 + N_2)n - \beta N_3 n. \tag{60}$$

We assume that the neutral component Γ_3 is fast and their residence time is short. The density of the fast neutrals is low,

$$N_3 \ll N_1, N_2, \tag{61}$$

so that they are not ionized. We approximate the continuity equations as

$$\frac{\mathrm{d}\Gamma}{\mathrm{d}z} = \beta(N_1 + N_2)n, \qquad \frac{\mathrm{d}\Gamma_1}{\mathrm{d}z} = -\beta_c N_1 n,$$
$$\frac{\mathrm{d}\Gamma_2}{\mathrm{d}z} = \beta_c N_2 n, \qquad \frac{\mathrm{d}\Gamma_3}{\mathrm{d}z} = \beta_c(N_1 + N_2)n. \tag{62}$$

From these approximated equations we derive the relation

$$\Gamma_3 = \frac{\beta_c}{\beta}\Gamma \gg \Gamma. \tag{63}$$

Relation (63) that follows equation (10) results in the flux of fast neutrals being larger than the plasma flux, expressing the fact that the force by the neutrals, rather than the ion momentum, balances the plasma pressure. The mass conservation is therefore approximated as

$$\Gamma_1 - \Gamma_2 + \frac{\beta_c}{\beta}\Gamma \cong \Gamma_m. \tag{64}$$

The slow neutrals are converted into fast neutrals and (at a smaller rate) ions. As said above, the densities of the slow neutral components are

$$N_1 = \frac{\Gamma_1}{v_a}, \qquad N_2 = \frac{\Gamma_2}{v_a}. \tag{65}$$

Equations (62) and (65) result, similarly to the collisionless case [30], in the relation

$$\Gamma_1(z)\Gamma_2(z) = \Gamma_0^2 = \text{const}. \tag{66}$$

We will now examine a system with a zero mass flow and a system with a net mass flow.

7. Zero mass flow

We start with a plasma confined between two walls at $z = \pm a$ which is symmetrical with respect to $z = 0$,

$$\Gamma_1(0) = \Gamma_2(0) = \Gamma_0, \qquad \Gamma_m = 0. \tag{67}$$

Equations (64) and (66) result in the relation

$$\Gamma_1(z) - \frac{\Gamma_0^2}{\Gamma_1(z)} + \frac{\beta_c}{\beta}\Gamma(z) = 0, \tag{68}$$

from which $\Gamma_1(z)$ is expressed as

$$\Gamma_1(z) = \frac{\beta_c}{2\beta}\left[-\Gamma(z) + \sqrt{\Gamma^2(z) + \left(\frac{2\beta\Gamma_0}{\beta_c}\right)^2}\right]. \tag{69}$$

Employing this expression for $\Gamma_1(z)$ and the relation $\Gamma_2(z) = \Gamma_1(z) + (\beta_c/\beta)\Gamma(z)$, we write the approximated neutral density as

$$N(z) \cong N_1(z) + N_2(z) = \frac{\Gamma_1(z) + \Gamma_2(z)}{v_a}$$
$$= \frac{\beta_c}{v_a\beta}\sqrt{\Gamma^2(z) + \left(\frac{2\beta\Gamma_0}{\beta_c}\right)^2}. \tag{70}$$

The equation for Γ in equations (62) becomes

$$\frac{\mathrm{d}\Gamma_n}{\mathrm{d}\xi} = P_n\sqrt{\Gamma_n^2(\xi) + B_c^2}\sqrt{1 - \Gamma_n^2} \tag{71}$$

in which

$$B_c \equiv \frac{2\beta\Gamma_0}{\beta_c\Gamma_a}, \qquad P_n \equiv \frac{\beta_c\Gamma_a a}{v_a c}\left(\frac{\beta_c}{\beta}\right)^{1/2}, \qquad \xi \equiv \frac{z}{a}. \tag{72}$$

It is convenient to write the last equation in the form

$$\frac{\mathrm{d}\theta}{\mathrm{d}\xi} = P_n\sqrt{\sin^2\theta + B_c^2}, \tag{73}$$

where

$$\sin\theta \equiv \Gamma_n. \tag{74}$$

The solution of the equation is

$$\int_0^\theta \frac{\mathrm{d}\theta'}{\sqrt{\sin^2\theta' + B_c^2}} = P_n\xi. \tag{75}$$

Integrating this equation we obtain the relation

$$\int_0^{\pi/2} \frac{\mathrm{d}\theta}{\sqrt{\sin^2\theta + B_c^2}} = P_n. \tag{76}$$

The case of low neutral depletion corresponds to $B_c \gg 1$. In that case $\pi/2 = B_c P_n = (2\Gamma_0 a/v_a c)(\beta\beta_c)^{1/2}$ as in the case of a uniform plasma density. The more interesting case is of strong neutral depletion, when $B_c \ll 1$. We estimate the value of the integral (76) as we did in [30]. We choose b such that $B_c \ll b \ll \pi/2$ and split the integral into two parts, one in the interval $[0, b]$ and the second in the interval $[b, \pi/2]$. In the first integral we approximate

$$\int_0^b \frac{\mathrm{d}\theta'}{\sqrt{(\theta')^2 + B_c^2}} = \ln\left(\frac{b + \sqrt{b^2 + B_c^2}}{B_c}\right) \cong \ln\left(\frac{2b}{B_c}\right). \tag{77}$$

The second integral is approximated as

$$\int_b^{\pi/2} \frac{\mathrm{d}\theta'}{\sin\theta'} = \frac{1}{2}\ln\frac{1 + \cos b}{1 - \cos b} \cong \ln\frac{2}{b}. \tag{78}$$

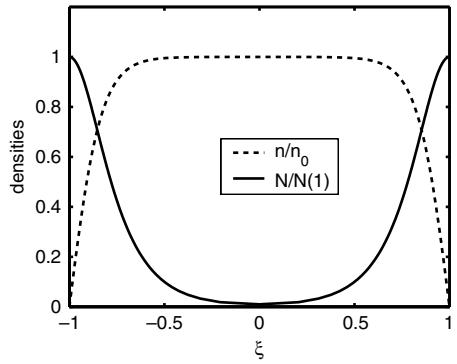

Figure 3. Plasma and neutral-gas normalized densities for a dominant neutral pumping. No mass flow. Here $B_c^2 = 0.0001$ and the neutral depletion is $D = 99$.

The sum of the two integrals turns out to be

$$\ln\left(\frac{4}{B_c}\right) = P_n \Longrightarrow B_c = 4\exp\left(-P_n\right). \tag{79}$$

The neutral depletion has been defined in equation (42). Expressing the neutral-gas densities at the boundary and at the center through equation (70), we find that

$$D = \frac{\sqrt{1+B_c^2}}{B_c} - 1, \tag{80}$$

and the large neutral depletion when $B_c \ll 1$ turns out to be

$$D \cong \frac{1}{B_c} \cong \frac{\exp P_n}{4}. \tag{81}$$

Figure 3 shows the profiles of the plasma and neutral-gas densities between the walls, for a case neutral pumping. In the following section we examine neutral pumping in an open system with a net mass flow.

8. Open system

The second configuration we analyze for a neutral flow affected by charge-exchange collisions is of a plasma produced between a wall at $z = 0$ and an open boundary at $z = a$ through which gas and plasma are free to leave the system. Gas is injected at $z = 0$ and the net particle flow density is Γ_m. Because of the free boundary there is no backward slow component of the gas,

$$\Gamma_2(z) = 0. \tag{82}$$

The conservation of particles is expressed as

$$\Gamma_\mathrm{m} = \Gamma(z) + \Gamma_1(z) + \frac{\beta_\mathrm{c}}{\beta}\Gamma(z) \cong \Gamma_1(z) + \frac{\beta_\mathrm{c}}{\beta}\Gamma(z), \tag{83}$$

and the neutral density

$$N(z) \cong \frac{\Gamma_1(z)}{v_\mathrm{a}}. \tag{84}$$

The plasma continuity equation becomes

$$\frac{\mathrm{d}\Gamma_\mathrm{n}}{\mathrm{d}\xi} = \alpha_o^{1/2}\left(1 - \eta_\mathrm{m}\Gamma_\mathrm{n}\right)\sqrt{1-\Gamma_\mathrm{n}^2}, \tag{85}$$

where

$$\eta_\mathrm{m} \equiv \frac{\beta_\mathrm{c}\Gamma_a}{\beta\Gamma_\mathrm{m}}, \qquad \alpha_o^{1/2} \equiv \frac{(\beta\beta_\mathrm{c})^{1/2}\Gamma_\mathrm{m}a}{cv_\mathrm{a}}, \qquad \xi \equiv \frac{z}{a}. \tag{86}$$

Here $\alpha_o^{1/2}$ is equivalent to $\alpha_L^{1/2}$ of section 5. Also, η_m, the ratio of the flux density of accelerated neutrals $(\beta_\mathrm{c}/\beta)\Gamma_a$ to the net mass flow density Γ_m, is appropriately called propellant utilization when such a configuration is employed as a thruster. Note also that $\eta_\mathrm{m} = 2/B_c$. Equation (85) can be written as

$$\frac{\mathrm{d}\theta}{\mathrm{d}\xi} = \alpha_o^{1/2}\left(1 - \sin\theta_0 \sin\theta\right), \tag{87}$$

where

$$\sin\theta \equiv \Gamma_\mathrm{n} \qquad \sin\theta_0 \equiv \eta_\mathrm{m}. \tag{88}$$

This equation is identical to the equation in [24] and to the equations in section 5. The equation is integrated to

$$\frac{1}{\cos(\theta_0)}\operatorname{arccot}\left(\frac{\sin\theta - \sin\theta_0}{\cos\theta\cos\theta_0}\right) = -\alpha_o^{1/2}\xi + A, \tag{89}$$

in which A is a constant. With the boundary conditions

$$\xi = 0 \qquad \sin\theta = -1, \qquad \xi = 1 \qquad \sin\theta = 1, \tag{90}$$

we find that $A = \pi$ and

$$\alpha_o^{1/2} = \frac{\pi}{\cos\theta_0}. \tag{91}$$

When neutral depletion is small θ_0, $\eta_\mathrm{m} \ll 1$ and $\alpha_o^{1/2} = \pi$ (a factor of 2 difference from the previous case is because here a and not $2a$ is the distance between the plasma boundaries). Equation (91) is written explicitly as

$$\beta\beta_\mathrm{c}\left(\frac{a\Gamma_\mathrm{m}}{v_\mathrm{a}c}\right)^2\left[1 - \left(\frac{\beta_\mathrm{c}\Gamma_a}{\beta\Gamma_\mathrm{m}}\right)^2\right] = \beta\beta_\mathrm{c}\left(\frac{a\Gamma_\mathrm{m}}{v_\mathrm{a}c}\right)^2\left(1-\eta_\mathrm{m}^2\right) = \pi^2. \tag{92}$$

We can define, similarly to what we did in [30], characteristic ionization and collisional mean free paths,

$$\lambda_\mathrm{ion} \equiv \frac{v_\mathrm{a}c}{\beta\Gamma_\mathrm{m}} \qquad \lambda_c \equiv \frac{v_\mathrm{a}c}{\beta_\mathrm{c}\Gamma_\mathrm{m}}, \tag{93}$$

and write equation (91) or (92) as

$$1 - \eta_\mathrm{m}^2 = \frac{\pi^2\lambda_\mathrm{ion}\lambda_c}{a^2}. \tag{94}$$

The profile of the normalized plasma flux ($\Gamma_\mathrm{n} = \sin\theta$) is then

$$\frac{\sin\theta - \sin\theta_0}{\cos\theta\cos\theta_0} = \frac{\Gamma_\mathrm{n} - \eta_\mathrm{m}}{\sqrt{1-\Gamma_\mathrm{n}^2}\sqrt{1-\eta_\mathrm{m}^2}} = \cot[\pi(-\xi)]. \tag{95}$$

The other variables are expressed as

$$n_\mathrm{n} = \sqrt{1-\Gamma_\mathrm{n}^2} \qquad N = \frac{\Gamma_\mathrm{m}\left(1 - \eta_\mathrm{m}\Gamma_\mathrm{n}\right)}{v_\mathrm{a}}. \tag{96}$$

We define the rate of neutral depletion equivalently to what we did in the previous case of no mass flow as

$$D \equiv \frac{N(z=0) - N(z=a)}{N(z=a)}. \tag{97}$$

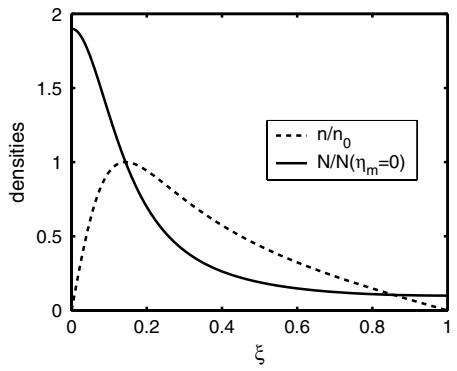

Figure 4. Plasma and neutral-gas normalized densities for a dominant neutral pumping. An open system and a net mass flow to the right. The propellant utilization is $\eta_m = 0.9$ and correspondingly the neutral depletion is $D = 18$.

Since $N(z = 0) = \Gamma_m(1 + \eta_m)/v_a$ and $N(z = a) = \Gamma_m(1 - \eta_m)/v_a$ we obtain that

$$D = \frac{2\eta_m}{1 - \eta_m}. \tag{98}$$

Figure 4 shows the plasma and neutral-gas normalized densities for an open system in which neutral pumping is dominant.

The use of such a configuration for a thruster has the advantage that the thrust is delivered mostly to neutrals. Sheath losses, which are a major source of inefficiency in collisionless plasmas [30], are minimal in this case. The analysis of the neutral dynamics in the dominant neutral pumping regime presented here does not provide us with an accurate enough estimate of the efficiency. Let us assume that the source of energy for thrust is the energy gained by the ions while they cross the potential drop across the plasma. Let us also assume that all this energy is delivered to the neutrals as directed kinetic energy. The losses include half of the energy that is wasted at the backwall, the energy cost for ionization ε_c and the energy losses at the sheath [4, 30]. The efficiency can be written as

$$\eta = \frac{e\Delta\varphi}{\varepsilon_c(T) + 2T + 0.25T[1 + \ln(m/2\pi m_e)] + 2e\Delta\varphi}. \tag{99}$$

This efficiency can be estimated once the electron temperature and plasma potential are evaluated.

9. Summary

In this paper we have analyzed how energizing the neutrals by a collisional plasma affects the neutral depletion and the plasma steady state. When neutrals are thermalized their gain of energy from the plasma results in a temperature increase. That temperature increase crucially depends on heat conductivity. We showed that if the heat conductivity is low the increase in neutral temperature can be significant and thus can result in a large neutral depletion even if the plasma pressure is relatively small. We then analyzed neutral pumping, a neutral depletion that follows the production of fast neutrals through charge-exchange collisions. Dominant neutral pumping was examined both in a closed system with no net mass flow and in an open system of a finite mass flow.

Acknowledgments

The author is grateful to Professor M Lieberman, Professor N Hershkowitz, G Makrinich and an anonymous referee for helpful comments. This research was partially supported by the Israel Science Foundation (Grant no. 864/07).

References

[1] Schottky W 1924 *Phys. Z.* **25** 635
[2] Forrest J R and Franklin R N 1966 *Br. J. Appl. Phys.* **17** 1569
Franklin R N 1976 *Plasma Phenomena in Gas Discharges* (Oxford: Clarendon)
[3] Godyak V A 1986 *Soviet Radio Frequency Discharge Research* (Falls Church: Delphic Associates)
[4] Lieberman M A and Lichtenberg A J 1994 *Principles of Plasma Discharges and Materials Processing* (New York: Wiley)
[5] Fruchtman A, Makrinich G and Ashkenazy J 2005 Two-dimensional equilibrium of a low temperature magnetized plasma *Plasma Sources Sci. Technol.* **14** 152
[6] Sternberg N, Godyak V and Hoffman D 2006 Magnetic field effects on gas discharge plasmas *Phys. Plasmas* **13** 063511
[7] Allen J E and Thonemann P C 1954 Current limitation in the low pressure mercury arc *Proc. Phys. Soc.* B **67** 768
[8] Caruso A and Cavaliere A 1964 The low pressure discharge in the strong ionization regime *Br. J. Appl. Phys.* **15** 1021
[9] Stangeby P C and Allen J E 1971 Current limitation in mercury vapour discharges: I. Theory *J. Phys. A: Gen. Phys.* **4** 108
Stangeby P C and Allen J E 1973 Current limitation in mercury vapour discharges: II. Experiment *J. Phys. D: Appl. Phys.* **6** 1373
[10] Valentini H B 1984 Theoretical description of gas discharges containing excited atoms at low pressures *J. Phys. D: Appl. Phys.* **17** 931
[11] Boswell R W and Porteous K 1987 Large volume, high density rf inductively coupled plasma *Appl. Phys. Lett.* **50** 1130
[12] Sudit I D and Chen F F 1996 Discharge equilibrium of a helicon plasma *Plasma Sources Sci. Technol.* **5** 43
[13] Gilland J, Breun R and Hershkowitz N 1998 Neutral pumping in a helicon discharge *Plasma Sources Sci. Technol.* **7** 416
[14] Degeling A W, Sheridan T E and Boswell R W 1999 Model for relaxation oscillations in a helicon discharge *Phys. Plasmas* **6** 1641
Degeling A W, Sheridan T E and Boswell R W 1999 Intense on-axis plasma production and associated relaxation oscillations in a large volume helicon source *Phys. Plasmas* **6** 3664
[15] Yun S, Taylor K and Tynan G R 2000 Measurement of radial neutral pressure and plasma density profiles in various plasma conditions in large-area high-density plasma sources *Phys. Plasmas* **7** 3448
[16] Tonnis E J and Graves D B 2002 Neutral gas temperatures measured within a high-density, inductively coupled plasma abatement device *J. Vac. Sci. Technol.* A **20** 1787
[17] Abada H, Chabert P, Booth J P, Robiche J and Gartry G 2002 Gas temperature gradients in a CF_4 inductive discharge *J. Appl. Phys.* **92** 4223
[18] Watts C and Hanna J 2004 Alfven wave propagation in a partially ionized plasma *Phys. Plasmas* **11** 1358
[19] Clarenbach B, Kramer M and Lorenz B 2007 Spectroscopic investigations of electron heating in a high-density helicon discharge *J. Phys. D: Appl. Phys.* **40** 5117

[20] Shimada M, Tynan G R and Cattolica R 2007 Neutral gas density depletion due to neutral gas heating and pressure balance in an inductively coupled plasma *Plasma Sources Sci. Technol.* **16** 193
[21] Keesee A M and Scime E E 2007 Neutral density profiles in argon helicon plasmas *Plasma Sources Sci. Technol.* **16** 742
[22] Aanesland A, Liard L, Leray G, Jolly J and Chabert P 2007 Direct measurements of neutral density depletion by two-photon absorption laser-induced fluorescence spectroscopy *Appl. Phys. Lett.* **91** 121502
[23] O'Connell D, Gans T, Crintea D L, Czarnetzki U and Sadeghi N 2008 Neutral gas depletion mechanisms in dense low-temperature argon plasmas *J. Phys. D: Appl. Phys.* **41** 035208
[24] Fruchtman A, Makrinich G, Chabert P and Rax J M 2005 Enhanced plasma transport due to neutral depletion *Phys. Rev. Lett.* **95** 115002
[25] Fruchtman A 2005 The effect of the magnetic field profile on the plume and on the plasma flow in the Hall thruster *IEPC-2005-068, 29th Int. Electric Propulsion Conf. (Princeton University, 31st October–4th November 2005)*
[26] Fruchtman A 2006 Neutral depletion and pressure balance in plasma *33rd EPS Conf. on Plasma Physics (Rome, Italy, 19–23 June 2006)* vol 30I (ECA) D-5.013
[27] Raimbault J-L, Liard L, Rax J-M, Chabert P, Fruchtman A and Makrinich G 2007 Steady-state isothermal bounded plasma with neutral dynamics *Phys. Plasmas* **14** 013503
[28] Maggs J E, Carter T A and Taylor R J 2007 Transition from Bohm to classical diffusion due to edge rotation of a cylindrical plasma *Phys. Plasmas* **14** 052507
[29] Liard L, Raimbault J-L, Rax J-M and Chabert P 2007 Plasma transport under neutral gas depletion conditions *J. Phys. D: Appl. Phys.* **40** 5192
[30] Fruchtman A 2008 Neutral depletion in a collisionless plasma *IEEE Trans. Plasma Sci.* **36** 403
[31] Charles C 2007 A review of recent laboratory double layer experiments *Plasma Sources Sci. Technol.* **16** R1
[32] Chang-Diaz F F 2000 The Vasimir rocket *Sci. Am.* **283** 90
[33] Manheimer W M and Fernsler R F 2001 Plasma acceleration by area expansion *IEEE Trans. Plasma Sci.* **29** 75
[34] Fruchtman A 2006 Electric field in a double layer and the imparted momentum *Phys. Rev. Lett.* **96** 065002
[35] Dunaevsky A, Raitses Y and Fisch N J 2006 Plasma acceleration from radio-frequency discharge in dielectric capillary *Appl. Phys. Lett.* **88** 251502
[36] Winglee R, Ziemba T, Giersch L, Prager J, Carscadden J and Roberson B R 2007 Simulation and laboratory validation of magnetic nozzle effects for the high power helicon thruster *Phys. Plasmas* **14** 063501
[37] Manente M, Carlsson J, Musso I, Bramanti C, Pavarin D and Angrilli F 2007 Numerical simulation of the Helicon Double Layer Thruster Concept *AIAA 2007-5312, 43rd AIAA/ASME/SAE/ASEE Joint Propulsion Conf. (Cincinnati, OH, 8–11 July 2007)*
[38] Chen F F 2007 Permanent magnet helicon source for ion propulsion Low Temperature Plasma Technology Laboratory, University of California Los Angeles *Report* LTP-709
[39] Batishchev O, Sinenian N, Celik M and Martinez-Sanchez M 2007 Development of the mini-helicon thruster at MIT *IEPC-2007-355, 30th Int. Electric Propulsion Conf. (Florence, Italy, 16–20 September 2007)*
[40] Palmer D, Akinli C, Williams L and Walker M L R 2007 Characterization of an annular helicon plasma source *IEPC-2007-202, 30th Int. Electric Propulsion Conf. (Florence, Italy, 16–20 September 2007)*
[41] Golant V, Zhilinsky A P, Sakharov I E and Brown S C 1980 *Fundamentals of Plasma Physics* (New York: Wiley)
[42] Murray J D 1984 *Asymptotic Analysis* (New York: Springer) chapter 2